

Hideyuki HASEGAWA · Hiroshi KANAI  
Nozomu HOSHIMIYA · Yoshiro KOIWA

## Evaluating the regional elastic modulus of a cylindrical shell with nonuniform wall thickness

Received: June 9, 2000 / Accepted: October 19, 2000

### Abstract

**Purpose.** For noninvasive diagnosis of atherosclerosis, we attempted to evaluate the elasticity of the arterial wall by measuring small changes in thickness caused by the heartbeat. The elasticity of the arterial wall has been evaluated noninvasively by measuring the change in diameter of the artery or the pulse-wave velocity; however, there is no method for noninvasively evaluating the elasticity of the arterial wall from changes in its thickness.

**Methods.** Employing the phased tracking method that we developed, changes in thickness of less than 100  $\mu\text{m}$  were measured in each regional area, which corresponded to the diameter of the ultrasonic beam.

**Results.** The elasticity of the arterial wall could be evaluated with better spatial resolution from the change in thickness than from the change in diameter of the artery or pulse-wave velocity. We therefore propose a method for evaluating the elastic modulus of an arterial wall of nonuniform wall thickness.

**Conclusions.** In basic experiments employing silicone rubber tubes with nonuniform wall thickness as arterial models, the elastic moduli of silicone rubber tubes were evaluated by measuring changes in wall thickness. These results confirm the value of the proposed method.

**Keywords** atherosclerosis · change in thickness of arterial wall · elastic modulus · small vibration on arterial wall

### Introduction

The steady increase in the incidence of myocardial infarction, cerebral infarction, and similar circulatory diseases mainly caused by atherosclerosis has become a serious problem. It is thus necessary to diagnose atherosclerosis in its early stage. Noninvasive evaluation of the elasticity of the arterial wall is useful for diagnosing atherosclerosis because atherosclerosis significantly changes the elasticity of the arterial wall.<sup>1</sup>

Previously proposed methods for noninvasively evaluating the elasticity of the arterial wall included measuring pulse-wave velocity and change in arterial diameter caused by the heartbeat. The elasticity of the arterial wall is evaluated using the Moens-Korteweg equation<sup>2</sup> from measured pulse-wave velocity or using the incremental elastic modulus,<sup>3</sup> the stiffness parameter,<sup>4</sup> and the pressure elastic modulus<sup>5</sup> from the change in diameter.

We set out to evaluate the regional elasticity of the arterial wall by ultrasonically measuring the small change in its thickness caused by the heartbeat.<sup>6</sup> From measurements of pulse-wave velocity and change in diameter, the average elasticity between several 10-cm intervals in the axial direction of the artery and that of the entire circumference, respectively, were evaluated. On the other hand, using the method proposed here,<sup>6,7</sup> the change in wall thickness can be measured in each regional area, which corresponds to an ultrasonic beam diameter of about 1 mm. If the elasticity of the arterial wall can be evaluated using the change in wall thickness, spatial resolution in measuring elasticity should prove superior to measuring pulse-wave velocity and change in diameter.

We propose a method for evaluating the elasticity of the arterial wall from the measured change in wall thickness produced by the heartbeat. Basic experiments employing silicone rubber tubes as arterial models show that the elasticity of the cylindrical shell can be evaluated using this method.

H. Hasegawa (✉) · H. Kanai · N. Hoshimiya  
Department of Electronic Engineering, Tohoku University Graduate  
School of Engineering, 05 Aramaki-aza-Aoba, Aoba-ku, Sendai  
980-8579, Japan

Y. Koiwa  
Department of Cardiovascular Medicine, Tohoku University  
Graduate School of Medicine, Sendai, Japan

## Measuring small changes in arterial wall thickness caused by the heartbeat

To determine the change in thickness of the arterial wall caused by the heartbeat, the velocity of the wall was measured as described below.<sup>6,7</sup>

As illustrated in Fig. 1, the received ultrasonic pulse has a phase delay,  $\theta(t)$ , corresponding to the bidirectional propagation between the ultrasonic probe and the target. The phase shift,  $\Delta\theta(t) = \theta(t + T) - \theta(t)$ , during one pulse repetition interval  $T$ , which corresponds to displacement of the target, is estimated from two consecutive echoes.

From the phase shift  $\Delta\theta(t)$ , the velocity of the target at time  $t + T/2$  is obtained as follows:

$$v\left(t + \frac{T}{2}\right) = -\frac{c}{2\omega_0} \frac{\Delta\theta(t)}{T} \quad (1)$$

where  $\omega_0$  and  $c$  are the central angular frequency of the ultrasound waves and the speed of sound, respectively. The speed of sound in tissue is assumed to be 1540 m/s.

The change in thickness,  $\Delta h(t)$ , of the arterial wall can be described by the difference between the displacement,  $x_{in}(t)$ , of the intimal side of the arterial wall and displacement,  $x_{ad}(t)$ , of the adventitial side. The change in thickness,  $\Delta h(t)$ , can thus be obtained by integrating the difference between the velocity,  $v_{in}(t)$ , of the intimal side and the velocity,  $v_{ad}(t)$ , of the adventitial side as follows.

$$\begin{aligned} \Delta h(t) &= x_{in}(t) - x_{ad}(t) \\ &= \int \{v_{in}(t) - v_{ad}(t)\} dt \end{aligned} \quad (2)$$

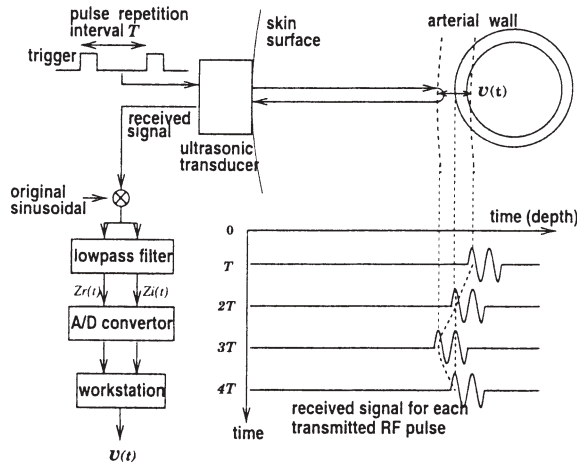


**Fig. 1.** Method used to measure velocity on the arterial wall. RF, radiofrequency

## Evaluating elastic modulus using small change in arterial wall thickness

When an artery can be assumed to be a cylindrical shell with uniform wall thickness

An artery without atherosclerotic plaque can be assumed to be a cylindrical shell with a wall of uniform thickness. Under such conditions, the incremental strain,  $\Delta\varepsilon_r(t)$ , in the radial direction at time  $t$  resulting from the pressure increment,  $\Delta p(t)$ , from the diastolic pressure,  $p_0$ , is expressed as follows<sup>8</sup>

$$\Delta\varepsilon_r(t) = \frac{\Delta\sigma_r(t)}{E_r} - \frac{\nu\Delta\sigma_\theta(t)}{E_\theta} - \frac{\nu\Delta\sigma_z(t)}{E_z} \quad (3)$$

where  $\nu$  is Poisson's ratio.  $E_r$ ,  $E_\theta$ , and  $E_z$  are elastic moduli in the radial, circumferential, and axial directions, respectively; and  $\Delta\sigma_r(t)$ ,  $\Delta\sigma_\theta(t)$ , and  $\Delta\sigma_z(t)$  are incremental stresses in the radial, circumferential, and axial directions, respectively. The second and third terms on the right side of Eq. (3) show decrements in radial strain resulting from circumferential strain  $\Delta\sigma_\theta(t)/E_\theta$  and axial strain  $\Delta\sigma_z(t)/E_z$ , which are determined by  $\nu$ , Poisson's ratio.

In vivo, the artery is strongly restricted in the axial direction.<sup>9</sup> Deformation of the artery in the axial direction can therefore be assumed to be negligible [ $\Delta\sigma_z(t)/E_z \approx 0$ ]. Equation (3) is thus approximated as follows:

$$\Delta\varepsilon_r(t) \approx \frac{\Delta\sigma_r(t)}{E_r} - \frac{\nu\Delta\sigma_\theta(t)}{E_\theta} \quad (4)$$

Because of the change in internal pressure,  $\Delta p(t)$ , caused by the heartbeat, the arterial wall is deformed as shown in Fig. 2. An enlarged view of the shaded area in Fig. 2 is shown in Fig. 3, in which the internal pressure and the external pressure (atmospheric pressure) at time  $t$  are defined by  $p_1(t)$  and  $p_2(t)$ , respectively.

Considering the balance of forces within a small region of the arterial wall, as shown in Fig. 3, forces on the x-axis, act on the arterial wall balance, as indicated by the fact that the shaded region is symmetrical with respect to the y-axis. The force in the y direction acting on a small region  $PP'$  is caused by the internal pressure,  $p_1(t)$ , and is expressed as follows.

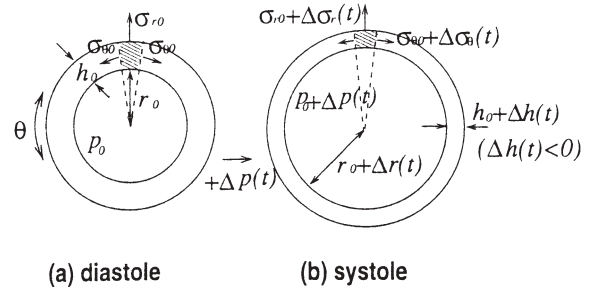


**Fig. 2.** Change in diameter and thickness of the arterial wall caused by change in internal pressure

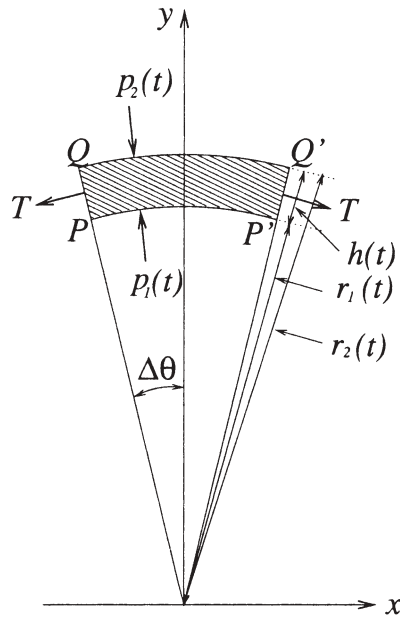


**Fig. 3.** Balance of forces in a small region of the arterial wall

$$p_1(t)\overline{PP'} = 2p_1(t)r_1(t)\sin\Delta\theta \quad (5)$$

Similarly, the force in the  $y$  direction acts on the small region  $QQ'$  because the external pressure,  $p_2(t)$ , is  $-2p_2(t)r_2(t)\sin\Delta\theta$ . Forces in the  $y$  direction caused by the internal pressure,  $p_1(t)$ , and the external pressure,  $p_2(t)$ , balance the  $y$ -axis component of tension  $T$ .

$$2p_1(t)r_1(t)\sin\Delta\theta - 2p_2(t)r_2(t)\sin\Delta\theta - 2T\sin\Delta\theta = 0 \quad (6)$$

Defining  $r_2(t)$  as  $r_1(t) + h(t)$  using the wall thickness,  $h(t)$ , tension,  $T$ , is expressed as follows.<sup>10</sup>

$$T = \{p_1(t) - p_2(t)\}r_1(t) - p_2(t)h(t) \quad (7)$$

When  $h(t) \approx 0$ , Eq. (7) is approximated by the following Laplace equation.

$$T \approx \{p_1(t) - p_2(t)\}r_1(t) \quad (8)$$

When tension,  $T$ , in Eq. (7) is divided by the wall thickness  $h(t)$ , stress,  $\sigma_\theta(t)$ , in the circumferential direction is expressed as follows.

$$\sigma_\theta = \frac{T}{h(t)} = \frac{r_1(t)}{h(t)}\{p_1(t) - p_2(t)\} - p_2(t) \quad (9)$$

Stress  $p_2(t)$  expands the arterial wall to counterbalance the atmospheric pressure  $p_2(t)$ . Therefore, by adding  $p_2(t)$  to Eq. (9), stress,  $\sigma_\theta(t)$ , in the circumferential direction is obtained by

$$\sigma_\theta(t) = \frac{r_1(t)}{h(t)}\{p_1(t) - p_2(t)\} \quad (10)$$

Measured internal pressure,  $p(t)$ , at time  $t$  corresponds to  $p_1(t) - p_2(t)$ . By defining  $\Delta r(t)$ ,  $\Delta h(t)$ , and  $\Delta p(t)$  as incre-

ments of the internal radius, wall thickness, and pressure from the inner radius,  $r_0$ , and wall thickness,  $h_0$ , at the diastolic pressure,  $p_0$ , respectively, Eq. (10) can be rewritten as follows.

$$\sigma_\theta(t) = \frac{r_0 + \Delta r(t)}{h_0 + \Delta h(t)}\{p_0 + \Delta p(t)\} \quad (11)$$

In systole, the internal radius increases as a result of the increased internal pressure [ $\Delta p(t) > 0$ ,  $\Delta r(t) > 0$ ]. Wall thickness, on the other hand, decreases.

Stress,  $\sigma_r(t)$ , in the radial direction is defined as the mean pressure between  $-p_1(t)$  at the inner surface of the wall and  $-p_2(t)$  at the outer surface.

$$\sigma_r(t) = -\frac{1}{2}\{p_1(t) + p_2(t)\} \quad (12)$$

As with Eq. (10), adding stress,  $p_2(t)$ , that balances the atmospheric pressure gives us stress,  $\sigma_r(t)$ , in the radial direction.

$$\sigma_r(t) = -\frac{1}{2}\{p_1(t) - p_2(t)\} = -\frac{1}{2}\{p_0 + \Delta p(t)\} \quad (13)$$

Given  $\Delta r(t)$  and  $\Delta h(t)$  sufficiently smaller than  $r_0$  and  $h_0$ , incremental stresses,  $\Delta\sigma_\theta(t)$  and  $\Delta\sigma_r(t)$ , in the circumferential and radial directions become increments from stresses  $r_0 p_0/h_0$  and  $-p_0/2$ , respectively, at diastolic pressure.

$$\begin{aligned} \Delta\sigma_\theta(t) &= \frac{r_0 + \Delta r(t)}{h_0 + \Delta h(t)}\{p_0 + \Delta p(t)\} - \frac{r_0}{h_0}p_0 \\ &\approx \frac{r_0}{h_0}\{p_0 + \Delta p(t)\} - \frac{r_0}{h_0}p_0 \\ &= \frac{r_0}{h_0}\Delta p(t) \geq 0 \end{aligned} \quad (14)$$

$$\begin{aligned} \Delta\sigma_r(t) &= -\frac{1}{2}\{p_0 + \Delta p(t)\} + \frac{1}{2}p_0 \\ &= -\frac{1}{2}\Delta p(t) \leq 0 \end{aligned} \quad (15)$$

When Eqs. (14) and (15) are substituted into Eq. (4), the ratio  $\Delta p(t)/\Delta\varepsilon_r(t)$  of the incremental pressure to the incremental strain in the radial direction can be described as follows, with the arterial wall assumed to be incompressible ( $\nu = 0.5$ ).<sup>11</sup>

$$\frac{\Delta p(t)}{\Delta\varepsilon_r(t)} = -\frac{2}{\left(\frac{1}{E_0} \frac{r_0}{h_0} + \frac{1}{E_r}\right)} < 0 \quad (16)$$

Equation (16) can then be expressed in the following form.

$$E_0 = \frac{1}{2}\left(\frac{r_0}{h_0} + \frac{E_0}{E_r}\right)\frac{\Delta p(t)}{-\Delta\varepsilon_r(t)} \quad (17)$$

The circumferential elastic modulus,  $E_\theta$ , in Eq. (17) cannot be derived when  $E_\theta/E_r$  is unknown. To obtain  $E_\theta$

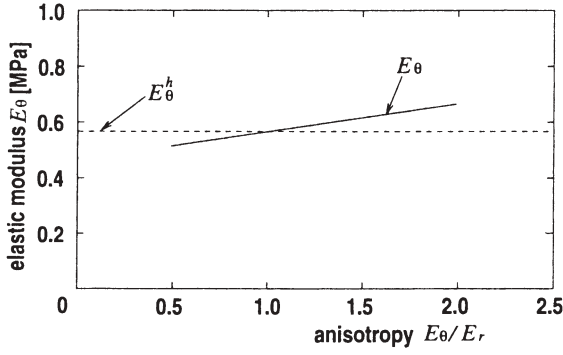


**Fig. 4.** Relation between elastic modulus,  $E_0$ , obtained by Eq. (17) and anisotropy  $E_r/E_0$ . Broken line shows the elastic modulus,  $E_0^h$ , obtained by Eq. (18), which is derived by approximating  $E_r$  by  $E_0$

from incremental strain,  $\Delta\varepsilon_r(t) = \Delta h(t)/h_0$ , in the radial direction, the arterial wall must be assumed to be elastically isotropic ( $E_r \approx E_0$ ). Approximating  $E_r$  as  $E_0$  has the following effect. The circumferential elastic modulus,  $E_0^h$ , is defined by the following equation by approximating  $E_r$  as  $E_0$  using incremental strain  $\Delta\varepsilon_r(t)$ .

$$E_0^h = \frac{1}{2} \left( \frac{r_0}{h_0} + 1 \right) \frac{\Delta p(t)}{-\Delta\varepsilon_r(t)} \quad (18)$$

The solid line in Fig. 4 shows the elastic modulus,  $E_0$ , defined by Eq. (17) plotted as a function of  $E_r/E_0$ . The broken line shows the circumferential elastic modulus,  $E_0^h$  defined by Eq. (18).  $\Delta p(t)/\Delta\varepsilon_r(t)$  is assumed to be 200kPa, and the ratio,  $r_0/h_0$ , of the inner radius to wall thickness is determined as follows. Figure 5 shows the ratio,  $r_0/h_0$ , of 68 carotid arteries without atherosclerotic plaque measured using B-mode ultrasonography. The mean value of 4.7 is used as a typical value when calculating  $E_0$  and  $E_0^h$  in Fig. 4.

$E_r/E_0$  has been reported to equal 0.8 in vivo.<sup>9</sup> The error in  $E_0^h$  obtained by Eq. (18) from  $E_0$  obtained by Eq. (17) is about 3% when  $E_r/E_0 = 0.8$ . Approximating  $E_r$  as  $E_0$  thus does not significantly influence the diagnosis of atherosclerosis because the change in elasticity caused by atherosclerosis exceeds 200%.<sup>1</sup> This shows that Eq. (18) evaluates the elastic modulus of an arterial wall of uniform thickness using incremental strain,  $\Delta\varepsilon_r(t)$ , in the radial direction.

When an artery cannot be assumed to be a cylindrical shell of uniform wall thickness

Wall thickness becomes nonuniform and greater than that of the normal arterial wall when the artery contains atherosclerotic plaque. We divided atherosclerotic plaque into several layers ( $N$  layers) and calculated the elastic modulus of each layer to assess the spatial distribution of the elastic modulus.

We divided an arterial wall of thickness  $h_0$  into  $N$  layers as shown in Fig. 6 to study the balance of forces resulting from internal pressure,  $p_1(t)$ , and external pressure,  $p_2(t)$ , in the shaded region of Fig. 6. As shown in Fig. 7, we assume

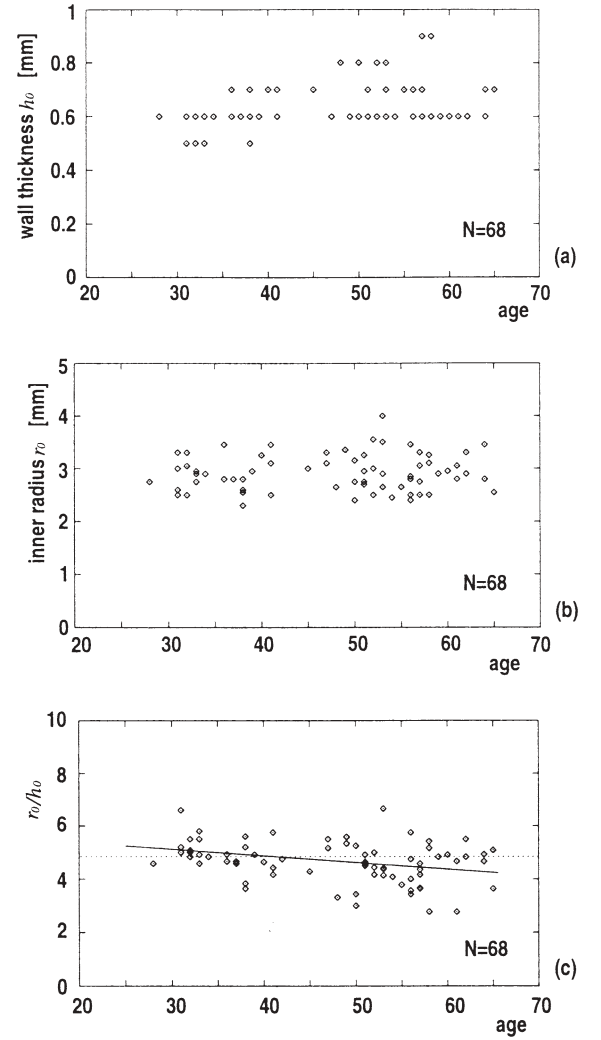


**Fig. 5.** Ratio of wall thickness,  $h_0$ , to inner radius,  $r_0$ , for 68 human common carotid arteries without atherosclerotic plaques. **a** Wall thickness  $h_0$ . **b** Inner radius  $r_0$ . **c** Ratio,  $r_0/h_0$ , of the internal radius to wall thickness

that pressure in the arterial wall changes linearly from  $p_1(t)$  to  $p_2(t)$  proportional to the distance from the internal surface of the arterial wall. Pressure,  $p_n(t)$ , at the internal radius of the  $n$ th ( $n = 1, 2, \dots, N$ ) layer is therefore described as follows.

$$p_n(t) = \frac{N - n + 1}{N} \{p_1(t) - p_2(t)\} + p_2(t) \quad (19)$$

As indicated by Eq. (6), the balance of forces in the  $y$  direction in the shaded region of Fig. 6 is expressed as

$$2p_n(t)\rho_n(t)\sin\Delta\theta - 2p_{n+1}(t)\rho_{n+1}(t)\sin\Delta\theta - 2T_n\sin\Delta\theta = 0 \quad (20)$$

where  $\rho_n(t)$  and  $T_n$  are the internal radius and the tension of the  $n$ th layer, respectively. By expressing  $\rho_{n+1}(t)$  by  $\rho_n(t) + h(t)/N$  using the thickness,  $h(t)/N$ , of a layer, the following equation is obtained in the same manner as was Eq. (7).

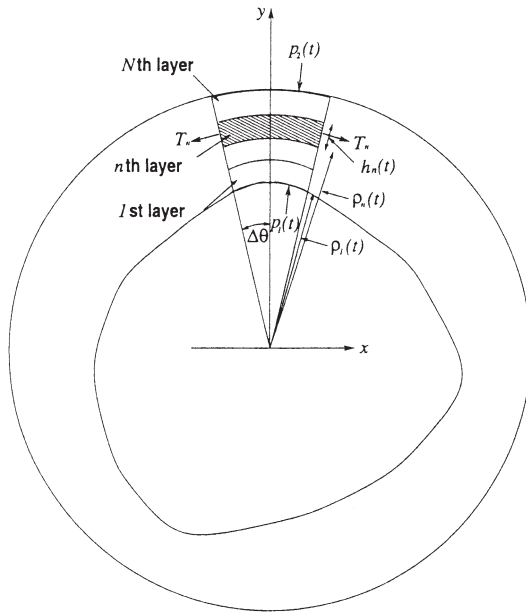


Fig. 6. Small region within the arterial wall

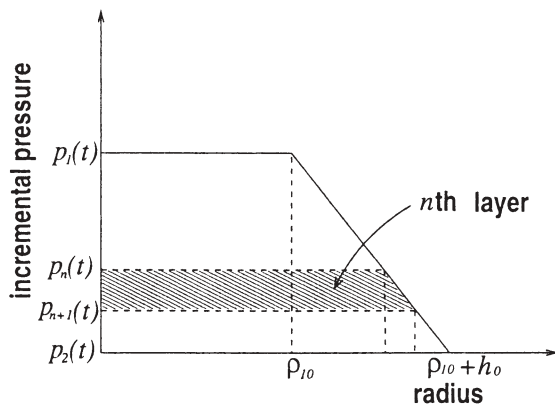


Fig. 7. Distribution of internal pressure in the radial direction

$$T_n = \{p_n(t) - p_{n+1}(t)\} \rho_n(t) - p_{n+1}(t) \frac{h(t)}{N} \quad (21)$$

The circumferential stress,  $\sigma_{\theta n}(t)$ , of the  $n$ th layer is obtained by dividing the tension,  $T_n$ , by the thickness,  $h(t)/N$ , of a layer.

$$\sigma_{\theta n}(t) = \frac{\rho_n(t)}{\left\{ \frac{h(t)}{N} \right\}} \frac{p_1(t) - p_2(t)}{N} - \frac{N-n}{N} \{p_1(t) - p_2(t)\} - p_2(t) \quad (22)$$

Increments in internal radius, layer thickness, and pressure from the internal radius  $\rho_{n0}$  and the layer thickness,  $h_0/N$ , at the diastolic pressure,  $p_0$ , are defined by  $\Delta\rho_n(t)$ ,  $\Delta h_n(t)$ , and  $\Delta p(t)$ , respectively. Adding the stress,  $p_2(t)$ , to counterbalance atmospheric pressure to Eq. (22), the following equation obtained, as with Eq. (11).

$$\sigma_{\theta n}(t) = \frac{\rho_{n0} + \Delta\rho_n(t)}{\left\{ \frac{h_0}{N} + \Delta h_n(t) \right\}} \frac{p_0 + \Delta p(t)}{N} - \frac{N-n}{N} \{p_0 + \Delta p(t)\} \quad (23)$$

As with Eq. (13), the radial stress,  $\sigma_r(t)$ , of the  $n$ th layer can be expressed as follows.

$$\sigma_r(t) = -\frac{1}{2} \{p_n(t) + p_{n+1}(t)\} + p_2(t) = -\frac{2N-2n+1}{2N} \{p_0 + \Delta p(t)\} \quad (24)$$

Equations (23) and (24) are confirmed in the appendix.

Given  $\Delta h_n(t) \ll h_0/N$  and  $\Delta\rho_n(t) \ll \rho_{n0}$ , incremental stresses,  $\Delta\sigma_{\theta n}(t)$  and  $\Delta\sigma_r(t)$ , in the circumferential and the radial directions of the  $n$ th layer can be obtained using the following equations as with Eqs. (14) and (15).

$$\begin{aligned} \Delta\sigma_{\theta n}(t) &= \frac{\rho_{n0} + \Delta\rho_n(t)}{\left\{ \frac{h_0}{N} + \Delta h_n(t) \right\}} \frac{p_0 + \Delta p(t)}{N} \\ &\quad - \frac{N-n}{N} \{p_0 + \Delta p(t)\} - \frac{\rho_{n0}}{\left( \frac{h_0}{N} \right)} \frac{p_0}{N} + \frac{N-n}{N} p_0 \\ &\approx \left\{ \frac{\rho_{n0}}{\left( \frac{h_0}{N} \right)} - (N-n) \right\} \frac{\Delta p(t)}{N} \end{aligned} \quad (25)$$

$$\begin{aligned} \Delta\sigma_r(t) &= -\frac{2N-2n+1}{2N} \{p_0 + \Delta p(t)\} + \frac{2N-2n+1}{2N} p_0 \\ &= -\frac{2N-2n+1}{2N} \Delta p(t) \end{aligned} \quad (26)$$

As with Eq. (4), the incremental strain,  $\Delta\varepsilon_r(t) = N \cdot \Delta h_n(t)/h_0$ , in the radial direction of the  $n$ th layer can be described as follows.

$$\Delta\varepsilon_r(t) = \frac{\Delta\sigma_r(t)}{E_m} - \nu \frac{\Delta\sigma_{\theta n}(t)}{E_{\theta n}} \quad (27)$$

where  $E_m$  and  $E_{\theta n}$  are elastic moduli in the radial and the circumferential directions, respectively. Assuming  $\nu$  equal 0.5 and substituting Eqs. (25) and (26) into Eq. (27) yields the following equation as with Eq. (17).

$$\begin{aligned} E_{\theta n} &= \left\{ \frac{\rho_{n0}}{\left( \frac{h_0}{N} \right)} - (N-n) + (2N-2n+1) \frac{E_{\theta n}}{E_m} \right\} \\ &\quad \times \frac{\Delta p(t)}{-2N\Delta\varepsilon_m(t)} \end{aligned} \quad (28)$$

By approximating  $E_{0n}/E_m$  as 1, the circumferential elastic modulus,  $E_{0n}^h$ , of the  $n$ th layer is obtained as follows :

$$E_{0n}^h \approx \frac{1}{2} \left\{ \frac{\rho_{n0}}{\left(\frac{h_0}{N}\right)} + (N - n + 1) \right\} \frac{\Delta p(t)}{-N\Delta\varepsilon_m(t)} \quad (29)$$

$$(n = 1, 2, \dots, N)$$

Substituting  $\rho_{n0} = \rho_{10} + (n - 1)h_0/N$  into Eq. (29) yields Eq. (30) when the incremental strain,  $\Delta\varepsilon_m(t)$ , is uniform in the radial direction ( $\Delta\varepsilon_m(t) = \Delta\varepsilon_{r0}(t)$ ).

$$E_{0n}^h \approx \frac{1}{2} \left\{ \frac{\rho_{10}}{\left(\frac{h_0}{N}\right)} + 1 \right\} \frac{\Delta p(t)}{-N\Delta\varepsilon_{r0}(t)} \quad (30)$$

$$(n = 1, 2, \dots, N)$$

Equation (30) shows that the elastic moduli of all layers are equivalent when the incremental strain is uniform. Furthermore, substituting  $\rho_{10} = r_0$  into Eq. (29) when there is only one layer makes it identical to Eq. (18).

$$E_{01}^h = \frac{1}{2} \left( \frac{r_0}{h_0} + 1 \right) \frac{\Delta p(t)}{-\Delta\varepsilon_{r1}(t)} = E_0^h \quad (31)$$

## Basic experiments using silicone rubber tubes

Using tubes with uniform wall thickness

The following basic experiments were carried out to confirm that the elastic modulus of a cylindrical shell of uniform wall thickness can be evaluated by Eq. (18). As illustrated in Fig. 8, the change in the wall thickness of the silicone rubber tube brought about by a change in internal pressure generated by an artificial heart was measured using ultrasound. The internal pressure and the drive signal of the artificial heart were acquired simultaneously. The size of the tube and the speed of sound in tube A are shown in Table 1.

The B-mode image of the silicone rubber tube obtained using standard diagnostic ultrasonic equipment is shown at the top of Fig. 9. The M-mode image shown in Fig. 9a was obtained by echoes reflected from a location on the tube. Figure 9b,c shows the drive signal of the artificial heart and internal pressure, respectively. Velocities,  $v_{ad}(t)$ , and  $v_{in}(t)$ , at the outside and inside of the anterior wall were derived, as shown in Fig. 9, from the received echoes, (Figs. 9d and 9e, respectively); and the change in wall thickness,  $\Delta h(t)$ , shown in Fig. 9f was obtained by integrating the difference between these two velocities.

Incremental strain,  $\Delta\varepsilon_r(t) = \Delta h(t)/h_0$ , in the radial direction was obtained from the change in wall thickness,  $\Delta h(t)$ , and thickness,  $h_0$ , of the wall shown in Table 1. Figure 10

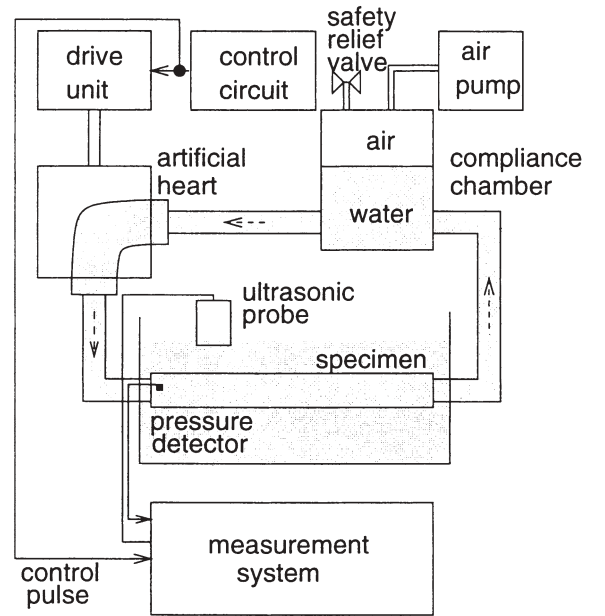


Fig. 8. Experimental setup for measuring the elastic modulus of the silicone rubber tube

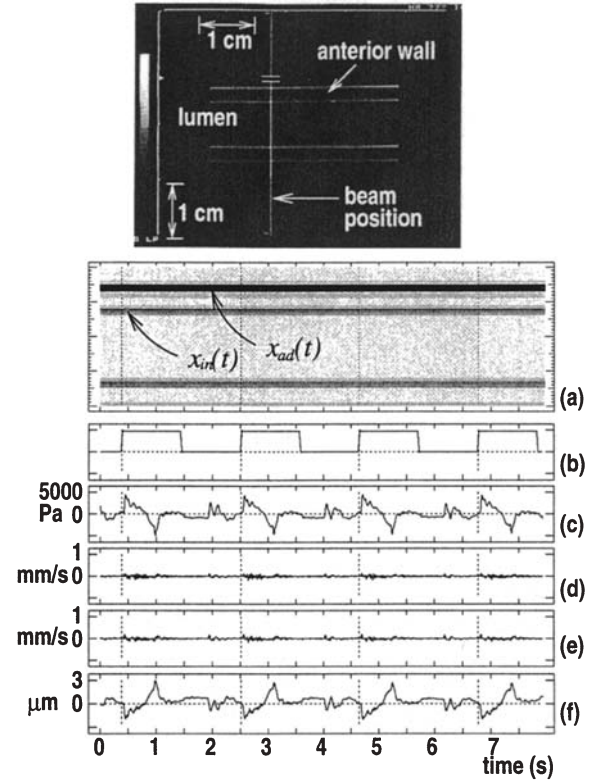
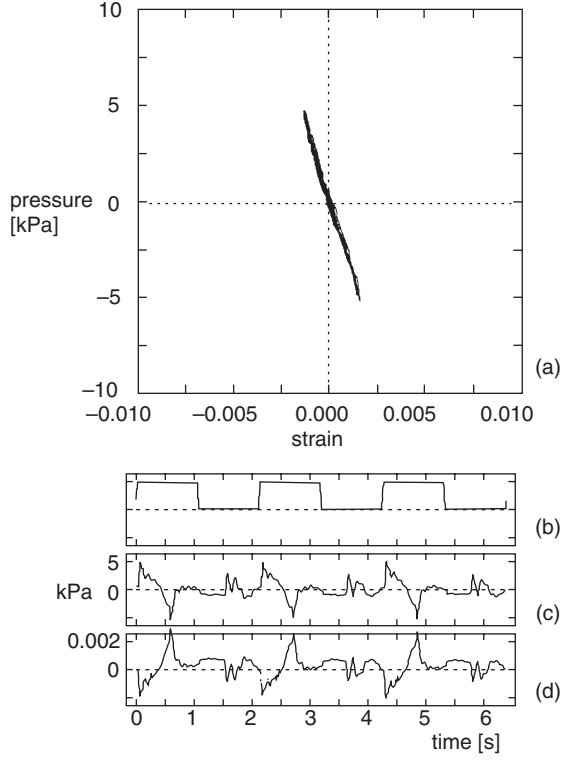


Fig. 9. Measuring change in thickness and the internal pressure. **Top** B-mode image of the silicone rubber tube obtained by standard ultrasonic diagnostic equipment. **a** M-mode image.  $x_{in}(t)$  and  $x_{ad}(t)$  show traces of tracking for the inner and external surfaces of the tube. **b** Drive signal of the artificial heart. **c** Internal pressure. **d** Velocity signal of the external surface  $v_{ad}(t)$ . **e** Velocity signal of the internal surface  $v_{in}(t)$ . **f** Change in wall thickness  $\Delta h(t)$

**Table 1.** Size, speed of sound, and elastic modulus of three silicone rubber tubes

Tube	Inner radius (mm)	Wall thickness (mm)	Speed of sound (m/s)	Incremental elastic modulus $E_{inc}$ (MPa)
Rubber tube A	4.0	1.5	992	5.7
Rubber tube B	7.5	2.5	1291	1.9
Rubber tube C	5.1	0.7	947	1.2



**Fig. 10.** Relation between internal pressure and strain in the radial direction in tube A. **a** Relation between internal pressure and strain in the radial direction. **b** Drive signal of the artificial heart. **c** Internal pressure. **d** Strain in the radial direction

shows the relation between incremental strain,  $\Delta\epsilon_r(t)$ , in the radial direction and incremental pressure  $\Delta p(t)$ . From the measured relation between incremental stress and incremental strain shown in Fig. 10a, the slope,  $\Delta p(t)/\Delta\epsilon_r(t)$ , of the stress-strain relation was obtained using the least-squares method; and the elastic modulus,  $E_0^h$ , was calculated as 5.8MPa by Eq. (18).

The elastic modulus of the tube was also measured by testing the relation between internal pressure and external diameter to validate the measured elastic modulus  $E_0^h$ . The experimental setup is shown in Fig. 11. This experiment tested the relation between internal pressure and external diameter by increasing the internal pressure by about 5 kPa using an air pump. The internal pressure and external diameter were measured using a pressure detector (NEC 9 E 02-P 16) and a laser line gauge (KEYENCE VG-035). Using the measured relation between internal pressure and external diameter, the elastic modulus in the circumferential direction was evaluated by the incremental elastic modulus,  $E_{inc}$ , as follows<sup>3</sup>

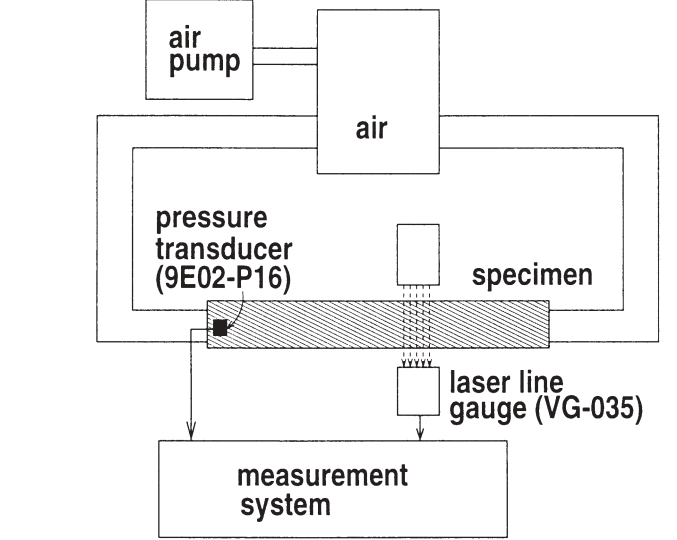


**Fig. 11.** System used to test the relation between the internal pressure and the external diameter

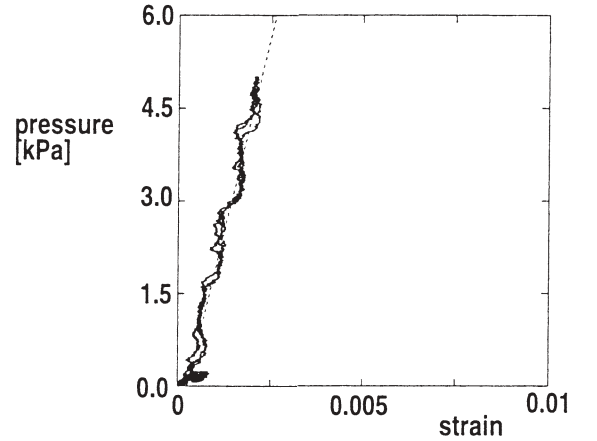


**Fig. 12.** Results of testing the relation between internal pressure and external diameter (tube A)

$$E_{inc} = \frac{3}{2} \frac{r_0^2 r_e}{r_e^2 - r_0^2} \frac{\Delta p(t)}{\Delta r_e(t)} \quad (32)$$

where  $r_e$  and  $\Delta r_e(t)$  refer to the original external radius and the change in external radius [ $\Delta r_e(t) > 0$ ].

Figure 12 shows the measured relation between incremental pressure,  $\Delta p(t)$ , and incremental strain  $\Delta r_e(t)/r_e$ . From the slope,  $r_e \cdot \Delta p(t)/\Delta r_e(t)$ , obtained using the least-

squares method, the incremental elastic modulus,  $E_{inc}$ , determined as 5.7 MPa by Eq. (32), agrees well with the elastic modulus,  $E_0^h$ , of 5.8 MPa measured by ultrasound.

Similar experiments were carried out on another silicone rubber tube with a different radius and wall thickness. The size and speed of sound of tube B are shown in Table 1. From experiments on tube B,  $E_0^h$  and  $E_{inc}$  were calculated to be 2.0 and 1.9 MPa, respectively, and are in close agreement. These results show that the elastic modulus of a cylindrical shell with uniform wall thickness can be evaluated by Eq. (18) when  $E_r$  can be approximated by  $E_0$ .

When the thickness of the tube is not uniform

Experiments similar to those previously described were conducted with a two-layered silicone rubber tube (tube C) with a nonconcentric cross section. Tube C served as a model of an artery with nonuniform wall thickness. The speed of sound of the silicone rubber tube was 947 m/s, and its size is described in Fig. 13. The two layers were made of the same material.

Figure 14c,d shows measured strains,  $\Delta\epsilon_{r1}(t)$  and  $\Delta\epsilon_{r2}(t)$ , in the radial direction in the inner and the outer layers, respectively. Figure 15a shows the relation between incremental pressure,  $\Delta p(t)$ , and incremental strain,  $\Delta\epsilon_{r1}(t)$ , in the radial direction of the inner layer. The elastic modulus,  $E_{01}^h$ , of the inner layer was determined to be 1.4 MPa by Eq. (29) from the slope of the relation between  $\Delta p(t)$  and  $\Delta\epsilon_{r1}(t)$  and the size of the tube. Similarly, Fig. 15b shows the relation between incremental pressure,  $\Delta p(t)$ , and incremental strain,  $\Delta\epsilon_{r2}(t)$ , in the radial direction of the outer layer. The elastic modulus,  $E_{02}^h$ , of the outer layer was determined to be 1.2 MPa by Eq. (29), and similar values of  $E_{0n}^h$  were obtained in these two layers.

To measure the incremental elastic modulus,  $E_{inc}$ , defined by Eq. (32), the relation between internal pressure and external diameter was tested of a silicone rubber tube with uniform wall thickness (tube D) made of the same material as tube C. The size of tube D is described in Table 1. Figure 16 shows the measured relationship between incre-

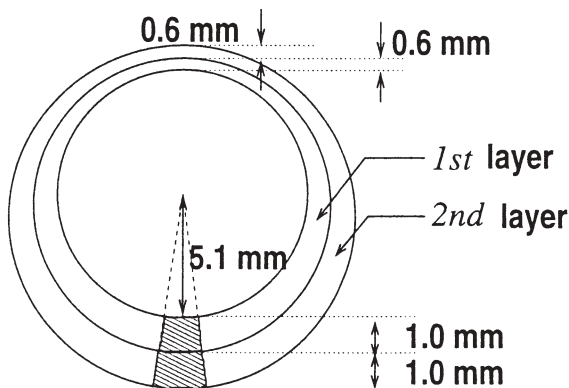


**Fig. 13.** Size of the cross section of silicone rubber tube C. The measure region is shaded

mental pressure,  $\Delta p(t)$ , and incremental strain  $\Delta r_e(t)/r_e$ . It shows that the incremental elastic modulus,  $E_{inc}$ , was evaluated to be 1.2 MPa by Eq. (32), agreeing closely with the measured values of elastic moduli,  $E_{01}^h$  and  $E_{02}^h$ , of tube C. These results are summarized in Table 2.

These results show that the elastic modulus in the circumferential direction can be evaluated approximately by Eq. (29), even when the shell is cylindrical and the thickness of its wall is not uniform.

## Conclusions

We propose a method for evaluating circumferential elastic modulus of a cylindrical shell by measuring change in its wall thickness resulting from change in its internal pressure. An artery without atherosclerotic plaques can be assumed to be a cylindrical shell of uniform wall thickness. However, wall thickness becomes nonuniform when the artery contains plaques. The proposed method provides an approach to measuring the regional elastic modulus of the arterial wall, even when the artery contains atherosclerotic plaques. In basic experiments, elastic moduli of silicone rubber tubes were evaluated using the proposed method and indicated that the elasticity of the arterial wall can be evaluated from ultrasonically measured changes in wall thickness. Such a method for noninvasively evaluating the elasticity of the arterial wall should prove useful for diagnosing atherosclerosis.

**Table 2.** Evaluation of elastic moduli of three silicone rubber tubes

Tube	$E_0^h$ (MPa)
Rubber tube A	5.8
Rubber tube B	2.0
Rubber tube X (first layer)	1.4
Rubber tube X (second layer)	1.2

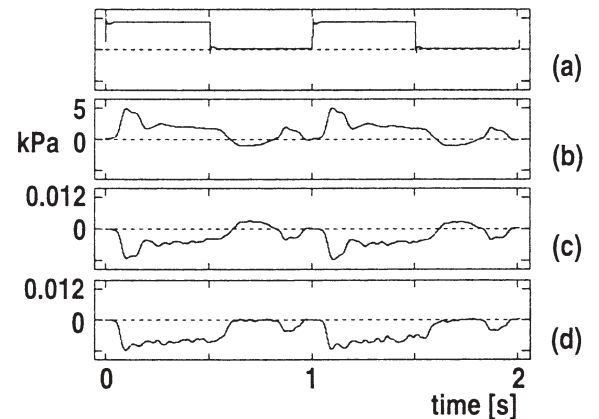


**Fig. 14.** Strain in the radial direction (tube C). **a** Drive signal of the artificial heart. **b** Internal pressure. **c** Strain in the radial direction of the inner layer. **d** Strain in the radial direction of the outer layer

**Fig. 15. a** Relation between internal pressure and strain in the radial direction of the inner layer in tube C. **b** Relation between internal pressure and strain in the radial direction of the outer layer of tube C

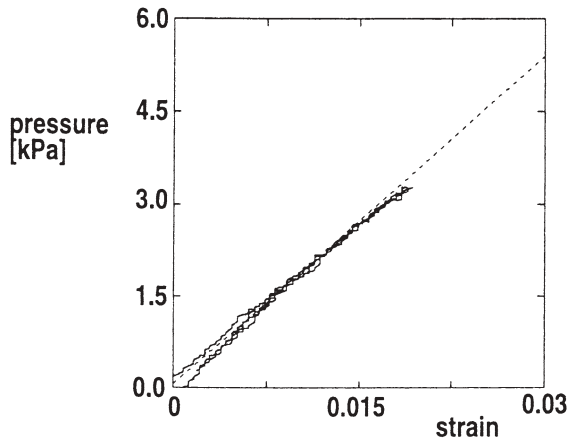
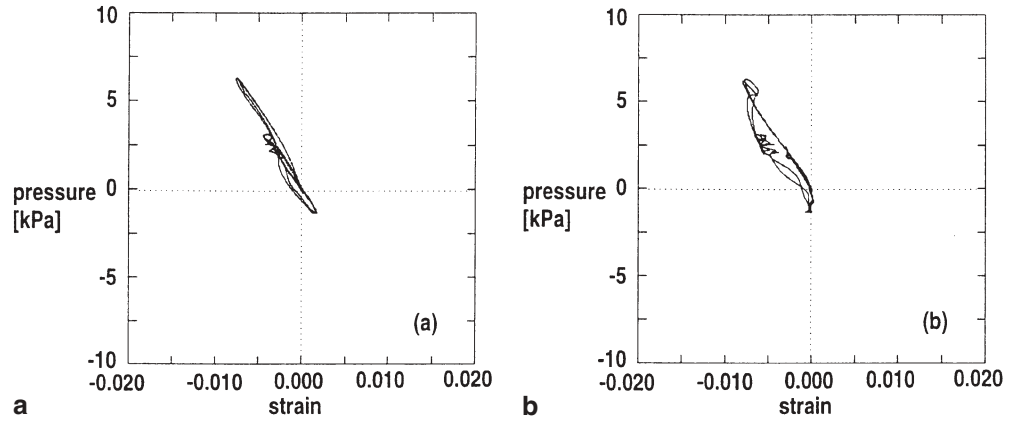


**Fig. 16.** Relation between internal pressure and external diameter in tube D

### Appendix: confirmation of definition of stresses $\sigma_{\theta n}(t)$ and $\sigma_m(t)$

Even when the arterial wall has uniform thickness, it can be divided into  $N$  layers. Mean radial stress obtained from the sum of the stresses of  $N$  layers should be identical to the radial stress of the entire wall defined by Eq. (13) as follows.

$$\sigma_r(t) = -\frac{1}{2}\{p_1(t) - p_2(t)\} \quad (33)$$

The mean radial stress,  $\sigma_r(t)$ , of  $N$  layers can be obtained as follows using Eq. (24).

$$\begin{aligned} & \frac{1}{N} \sum_{n=1}^N \left\{ -\frac{2N - 2n + 1}{2N} \{p_1(t) - p_2(t)\} \right\} \\ &= -\frac{1}{N} \frac{2N^2 - N(N + 1) + N}{2N} \{p_1(t) - p_2(t)\} \\ &= -\frac{1}{2} \{p_1(t) - p_2(t)\} \end{aligned} \quad (34)$$

Equation (34) turns out to be identical to Eq. (13).

In the same manner, from circumferential stresses,  $\sigma_{\theta n}(t)$  ( $n = 1, 2, \dots, N$ ), of  $N$  layers defined by Eq. (23), the mean circumferential stress,  $\sigma_{\theta}(t)$ , of the entire wall can be obtained by dividing the tension  $T = \sum_{n=1}^N T_n = \sum_{n=1}^N h(t)\sigma_{\theta n}(t)/N$  of the entire wall by the wall thickness,  $h(t)$ .

$$\begin{aligned} & \frac{1}{h(t)} \sum_{n=1}^N \frac{h(t)}{N} \sigma_{\theta n}(t) \\ &= \frac{1}{h(t)} \sum_{n=1}^N \frac{h(t)}{N} \left\{ \frac{p_n(t)}{\left(\frac{h(t)}{N}\right)} - (N - n) \right\} \frac{p_1(t) - p_2(t)}{N} \\ &= \frac{1}{h(t)} \sum_{n=1}^N \frac{h(t)}{N} \left\{ \frac{r_1(t) + \frac{h(t)}{N}(n - 1)}{\left(\frac{h(t)}{N}\right)} - (N - n) \right\} \\ &\quad \times \frac{p_1(t) - p_2(t)}{N} = \frac{1}{h(t)} \sum_{n=1}^N \frac{h(t)}{N} \left\{ \frac{r_1(t)}{\left(\frac{h(t)}{N}\right)} - (N - 2n + 1) \right\} \\ &\quad \times \frac{p_1(t) - p_2(t)}{N} = \frac{r_1(t)}{h(t)} \{p_1(t) - p_2(t)\} \end{aligned} \quad (35)$$

Equation (35) also turns out to be identical to Eq. (10).

Thus the radial and circumferential mean stresses of the entire wall defined by Eqs. (13) and (10) can be derived from stresses,  $\sigma_m(t)$  and  $\sigma_{\theta n}(t)$ , of each layer, theoretically confirming Eqs. (24) and (23).

---

**References**

1. Lee LT, Grodzinsky AJ, Frank EH, et al. Structure-dependent dynamic mechanical behavior of fibrous caps from human atherosclerotic plaques. *Circulation* 1991;83:1764–70.
2. Hallock P. Arterial elasticity in man in relation to age as evaluated by the pulse wave velocity method. *Arch Intern Med* 1934;54:770–98.
3. Bergel DH. The static elastic properties of the arterial wall. *J Physiol* 1961;156:445–57.
4. Hayashi K, Handa H, Nagasawa S, et al. Stiffness and elastic behavior of human intracranial and extracranial arteries. *J Biomech* 1980;13:175–84.
5. Peterson RH, Jensen RE, Parnell R. Mechanical properties of arteries in vivo. *Circ Res* 1960;8:622–39 (in Japanese).
6. Hasegawa H, Kanai H, Chubachi N, et al. Evaluation of the elastic modulus of the arterial wall by accurate noninvasive measurement of change in wall thickness. *J Med Ultrasonics* 1997;22:851–60 (in Japanese).
7. Kanai H, Sato M, Koiwa Y, et al. Transcutaneous measurement and spectrum analysis of heart wall vibrations. *IEEE Trans UFFC* 1996;43:791–810.
8. Patel DJ, Janicki JS, Vaishnav RN. Dynamic anisotropic viscoelastic properties of the aorta in living dogs. *Circ Res* 1973;32:93–107.
9. The Japan Society of Mechanical Engineers. *Mechanical Engineers' Handbook, Engineering, C6 Biotechnology and Medical Engineering*. Tokyo: Maruzen; 1988. p. 148 (in Japanese).
10. Oka S. *Rheology*. Tokyo: Shokabo; 1974. p. 308–36 (in Japanese).
11. Carew TE, Vaishnav RN, Patel DJ. Compressibility of the arterial wall. *Circ Res* 1968;23:61–8.